

Supplementary Information for:
**Catalytic Diversification Upon Metal Scavenging in a
Prebiotic Model for Formation of Tetrapyrrole Macrocycles**

Ana R. M. Soares, Dana R. Anderson, Vanampally Chandrashaker and Jonathan S. Lindsey

Table of Contents

Section	Topic	Page
I.	Metalation of uroporphyrin	S1-4
II.	Mass spectrometric characterization	S5-6
III.	Additional studies for metalation of uroporphyrin	S7-9
IV.	Effect of imidazole on metalations of uroporphyrin	S9-10
V.	Multicomponent analysis	S11-14
VI.	Dione–aminoketone reaction in the presence of each metal individually	S15-19
VII.	Examination of increased Mn(II)	S20-22
VIII.	Dione–aminoketone reaction in the presence of metals	S22-24

I. Metalation of uroporphyrin

Each reaction was performed using 2, 4 or 8 equivalents of each metal [Mg(II), Mn(II), Fe(II), Co(II), Ni(II), Cu(II), Zn(II) and Pd(II)] and was monitored by absorption spectroscopy after 1, 3 and 24 h (Figures S1-S3). Remarks in addition to those in the text concerning metalation of uroporphyrin in neutral aqueous solution are as follows:

- **Cu(II):** Two equivalents of Cu(II) gave complete metalation within 1 h, whereas 4 equivalents resulted in a decrease in the Soret and Q bands typical of aggregation.
- **Zn(II):** Two equivalents of Zn(II) gave complete metalation within 1 h, whereas an additional unknown band at ~600 nm was observed after 24 h. Four equivalents of Zn(II) resulted in a decrease in the Soret and Q bands typical of aggregation.
- **Pd(II):** Four equivalents of Pd(II) gave complete insertion within 3 h. An additional unknown band at ~600 nm was observed after 24 h.
- Heterogeneous mixtures were observed for reactions with 8 equivalents of Zn(II), Cu(II) or Ni(II). The heterogeneous mixtures consisted of an upper aqueous solution (supernatant) and precipitates on the bottom of the reaction vial. The heterogeneous samples were treated with DMF to obtain homogeneity. No significant changes were observed in the absorption spectra of the supernatant compared to those of samples treated with DMF.

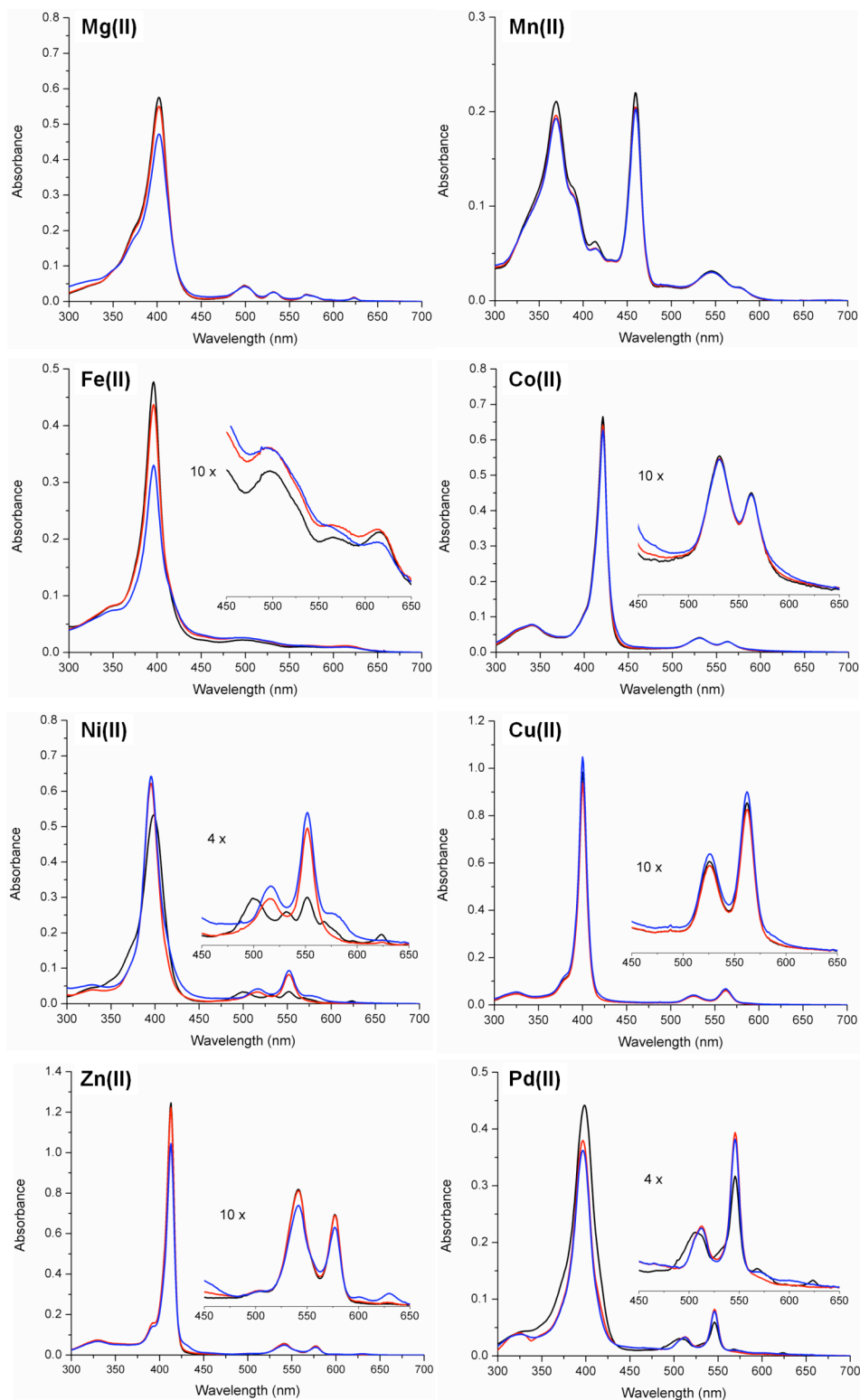


Figure S1. Absorption spectra for the metalation of uroporphyrin in aqueous solution in the presence of 2 equivalents of each metal individually (as indicated). Metalation was monitored after 1 h (black), 3 h (red) and 24 h (blue). Reaction in the presence of imidazole [(Co(II) and Fe(II)]. Spectra were acquired in DMF except for that in Fe(II), which was in DMSO.

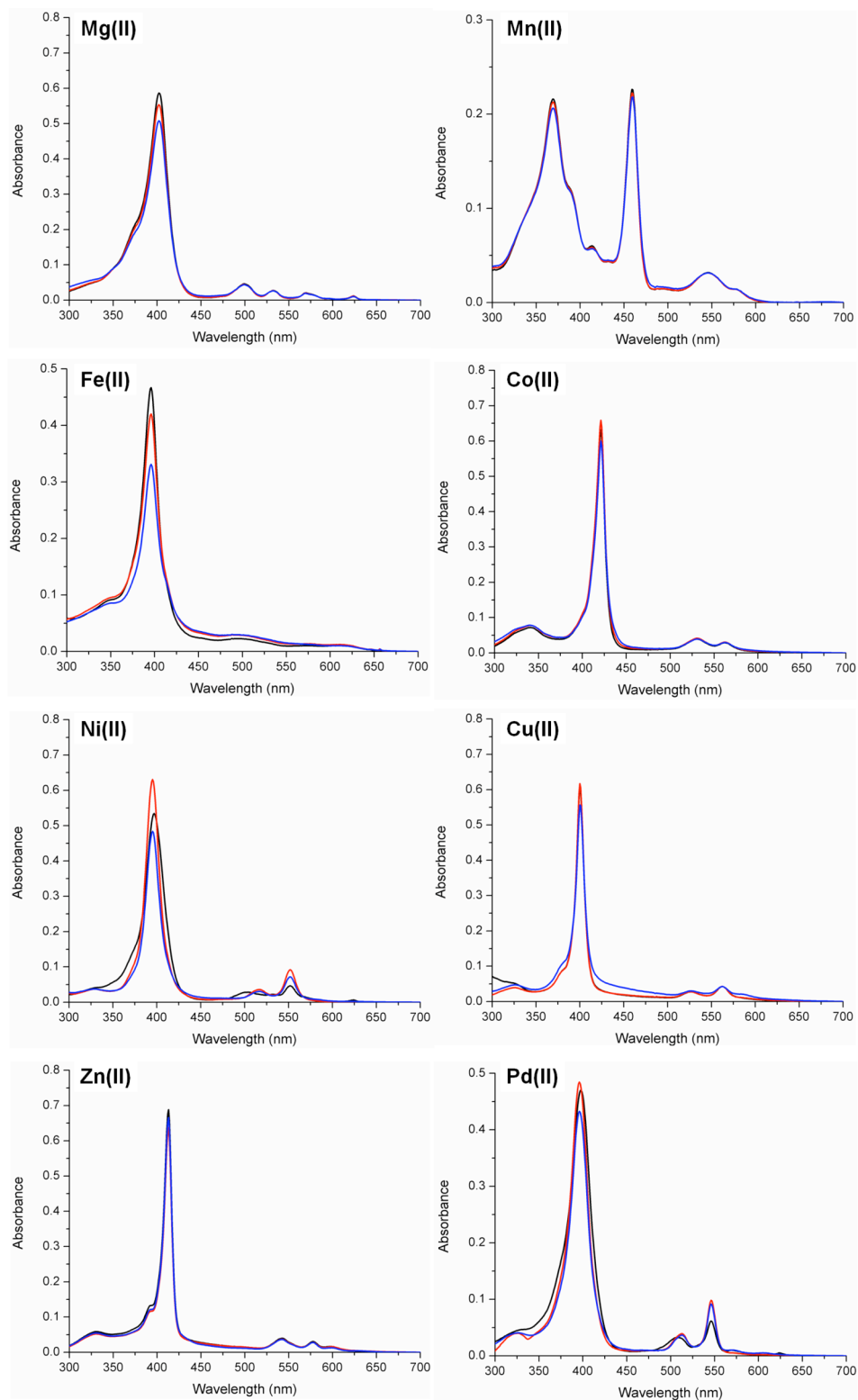


Figure S2. Absorption spectra for the metalation of uroporphyrin in aqueous solution in the presence of 4 equivalents of each metal individually (as indicated). Metalation was monitored after 1 h (black), 3 h (red) and 24 h (blue). Reaction in the presence of imidazole [(Co(II) and Fe(II)]. Spectra were acquired in DMF except for that in Fe(II), which was in DMSO.

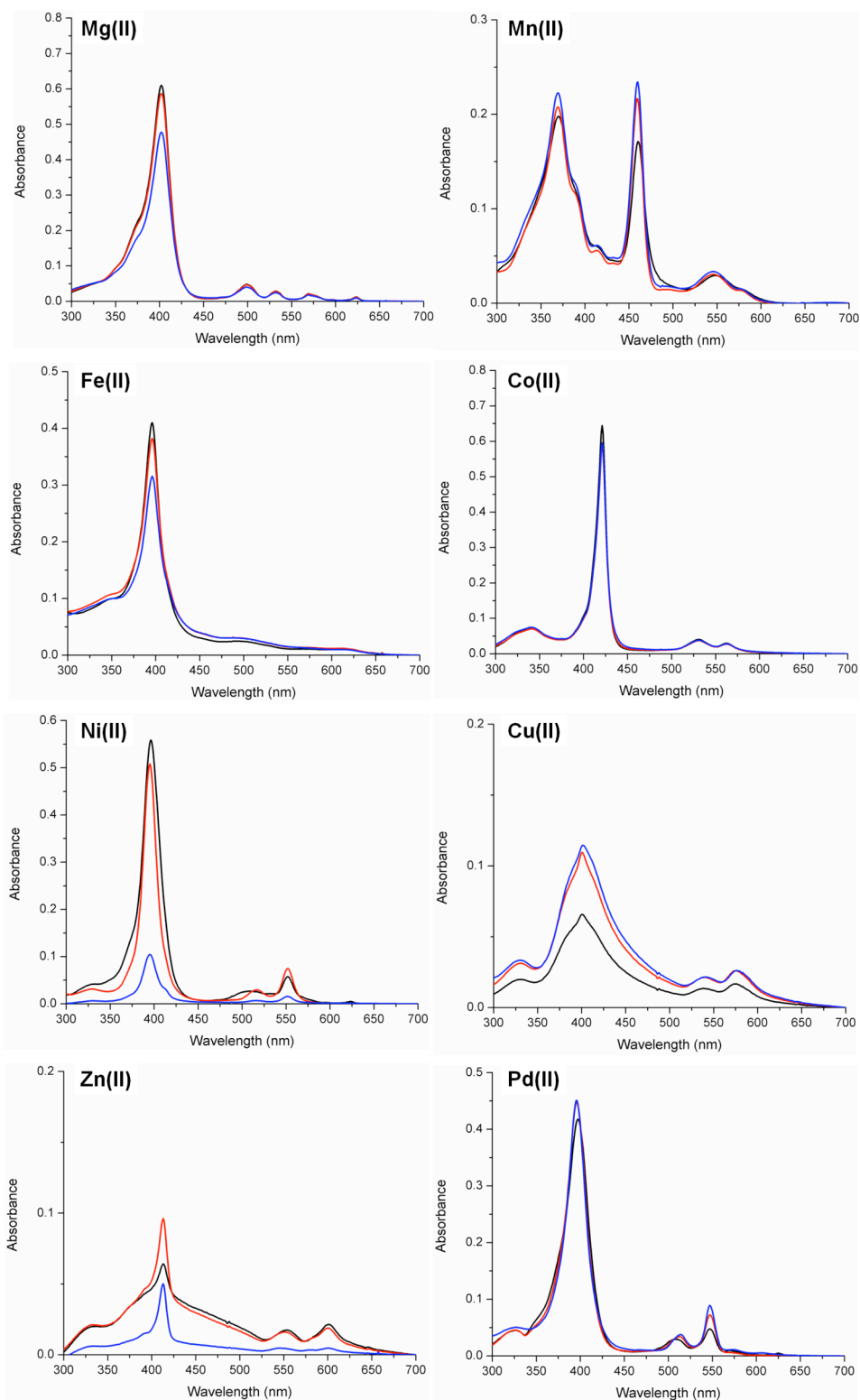


Figure S3. Absorption spectra for the metalation of uroporphyrin in aqueous solution in the presence of 8 equivalents of each metal individually (as indicated). Metal insertion was monitored after 1 h (black), 3 h (red) and 24 h (blue). Reaction in the presence of imidazole [(Co(II) and Fe(II)]. Spectra were acquired in DMF except for that in Fe(II), which was in DMSO.

II. Mass Spectrometric Characterization

MALDI-MS data were obtained using the crude reaction mixtures (Table S1). Representative spectra are displayed in Figure S4 for uroporphyrin (panel A), Zn(II)uroporphyrin (panel B), and Mn(III)uroporphyrin (panel C). The spectra for the Zn(II) and Mn(III) chelates are essentially devoid of peaks characteristic of free base uroporphyrin, as expected upon complete metalation. The spectrum for the zinc chelate displays the manifold of peaks due to the natural isotopic abundance of zinc; the manifold with $m/z = 847.08$ is attributed to a single decarboxylation (loss of CO_2H , -45 Da) of the Zn(II)porphyrin, likely of an acetic acid moiety given the greater propensity of acetic versus propionic acid in this regard.

Table S1. MALDI-MS data of each (metallo)uroporphyrin.

Compound	m/z obsd	m/z calcd	Formula (M)
Free base Uroporphyrin	831.21	$831.23 (\text{M} + \text{H})^+$	$\text{C}_{40}\text{H}_{38}\text{N}_4\text{O}_{16}$
Mn(III)Uroporphyrin	883.08	$883.15 (\text{M}^+)$	$\text{C}_{40}\text{H}_{36}\text{N}_4\text{O}_{16}\text{Mn}$
Fe(III)Uroporphyrin	884.08	$884.15 (\text{M}^+)$	$\text{C}_{40}\text{H}_{36}\text{N}_4\text{O}_{16}\text{Fe}$
Co(III)Uroporphyrin	887.07	$887.15 (\text{M}^+)$	$\text{C}_{40}\text{H}_{36}\text{N}_4\text{O}_{16}\text{Co}$
Ni(II)Uroporphyrin	886.07	$886.15 (\text{M}^+)$	$\text{C}_{40}\text{H}_{36}\text{N}_4\text{O}_{16}\text{Ni}$
Cu(II)Uroporphyrin	891.07	$891.14 (\text{M}^+)$	$\text{C}_{40}\text{H}_{36}\text{N}_4\text{O}_{16}\text{Cu}$
Zn(II)Uroporphyrin	892.08	$892.14 (\text{M}^+)$	$\text{C}_{40}\text{H}_{36}\text{N}_4\text{O}_{16}\text{Zn}$
Pd(II)Uroporphyrin	934.06	$934.12 (\text{M}^+)$	$\text{C}_{40}\text{H}_{36}\text{N}_4\text{O}_{16}\text{Pd}$

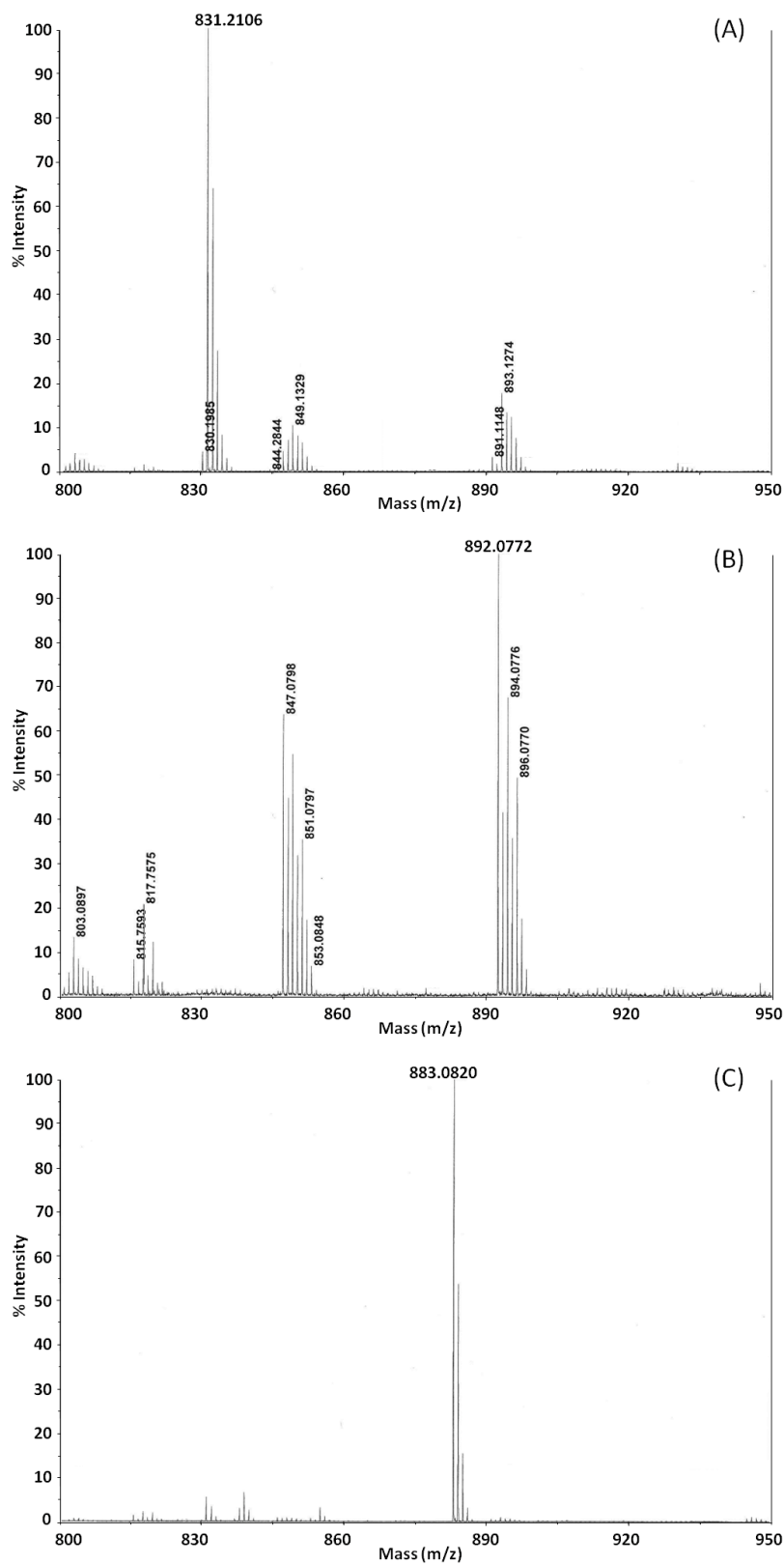


Figure S4. MALDI-MS data for free base uroporphyrin (A), Zn(II)uroporphyrin (B), and Mn(III)uroporphyrin (C) obtained by metalation of uroporphyrin in aqueous solution.

III. Additional studies for metalation of uroporphyrin with Mn(II), Fe(II) or Co(II)

Insertion of redox active metals such as manganese, iron and cobalt was also analyzed in the presence of a reducing agent (sodium dithionite). The absorption spectra for these reactions after 1 h are shown in Figure S5. We observed the following:

- (i) metalation with Mn(II) (panel A) yields Mn(III)uroporphyrin, showing two intense bands in the Soret band region (369 and 461 nm, black line), whereas reaction in the presence of sodium dithionite (5 mM) affords a mixture of Mn(II)uroporphyrin and Mn(III)uroporphyrin (red line). (In the cuvette, the concentration of porphyrin is 2.4×10^{-4} M and the concentration of sodium dithionite is 0.1 mM.) Additional treatment with 0.8 mM of sodium dithionite in the cuvette did not lead to further reduction of Mn(III)uroporphyrin;
- (ii) metalation with Fe(II) (panel B) gives Fe(III)uroporphyrin, showing the Soret band at 393 nm (black line), whereas reaction in the presence of sodium dithionite affords mainly Fe(II)uroporphyrin (a shoulder due to Fe(III) complex was still evident). Treatment with sodium dithionite in the cuvette gives exclusively Fe(II)uroporphyrin, showing the Soret band at 409 nm (red line). (In the cuvette, the concentration of porphyrin is 2.4×10^{-4} M and the concentration of sodium dithionite is 0.8 mM.);
- (iii) metalation with Co(II) (panel C) in the presence of imidazole yields a stable Co(III)uroporphyrin, showing the Soret band at 419 nm (black line), whereas reaction in the presence of dithionite gives Co(II)uroporphyrin, showing the Soret band at 409 nm (red line). (In the cuvette, the concentration of porphyrin is 2.4×10^{-4} M and the concentration of sodium dithionite is 0.1 mM.)

To confirm the formation of a Fe(III)porphyrin monomer instead of an μ -oxo dimer, an aliquot of the reaction was treated with pyridine or imidazole (Figure S6). We observed that treatment with either pyridine or imidazole led to spectral changes, which are typical of 6-coordinate complexes of Fe(III)porphyrins (black and red lines).

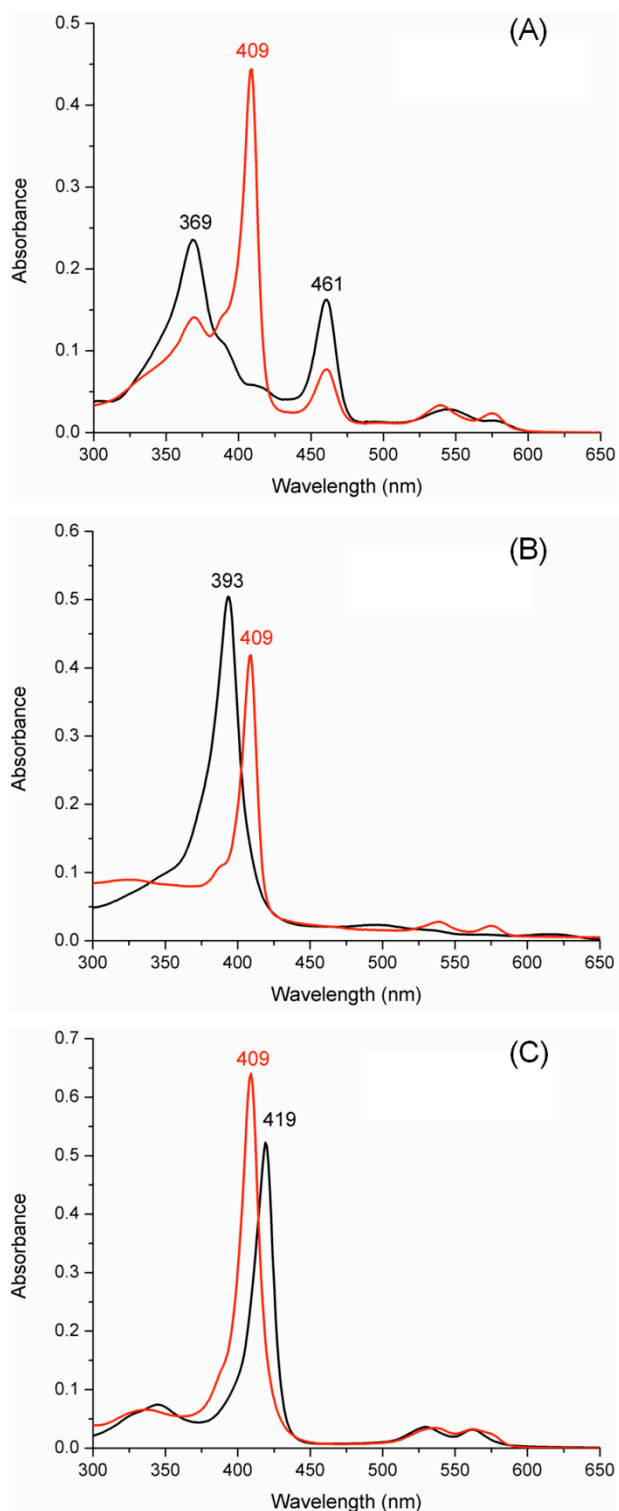


Figure S5. Absorption spectra (in 0.1 M MOPS buffer pH 7) for metalation of uroporphyrin with Mn(II), Fe(II) or Co(II). (A) Reaction with 2 equivalents of Mn(II) in the absence (black line) or presence of sodium dithionite (red line). (B) Reaction with 4 equivalents of Fe(II) in the absence (black line) or presence of sodium dithionite (red line). (C) Reaction with 2 equivalents of Co(II) in the presence of imidazole (black line) or sodium dithionite (red line).

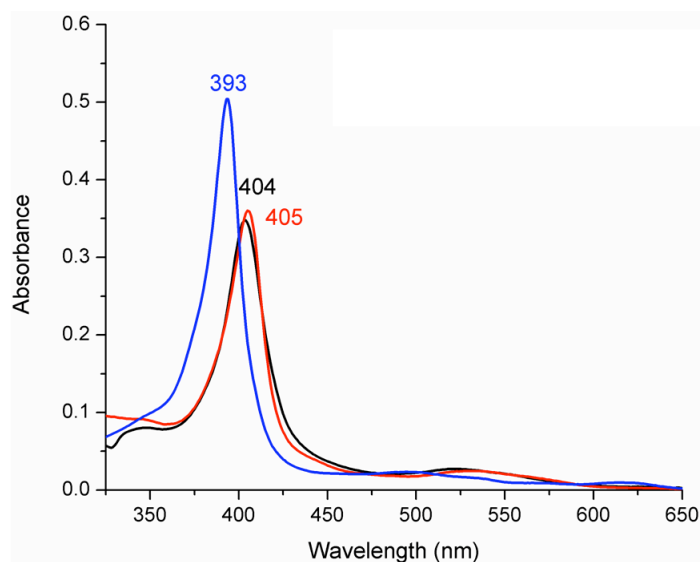


Figure S6. Absorption spectra for metalation of uroporphyrin with 4 equivalents of Fe(II). Spectra acquired in neutral aqueous solution (blue line), pyridine (black line) or in neutral aqueous solution containing imidazole (33 mM; red line).

IV. Effect of imidazole on metalations of uroporphyrin

The requirement of imidazole for the formation of stable Co(III)uroporphyrin, led us to study the metalation of uroporphyrin with each metal in the presence of imidazole. The reaction conditions employed are listed in Table 2 (main text) and the corresponding absorption spectra either in the absence or presence of imidazole are shown in Figure S7. No significant changes were observed for reactions in the presence versus absence of imidazole for most of the metallouroporphyrins [from metal salts Mn(II), Fe(II), Ni(II), Cu(II) and Zn(II)] and free base uroporphyrin. Exceptions were observed for (i) Co(II), which afforded a stable complex; and (ii) Pd(II), which reaction in the presence of imidazole resulted in exclusively free base uroporphyrin; this reaction was monitored for 4 h and no changes in the absorption spectrum were detected.

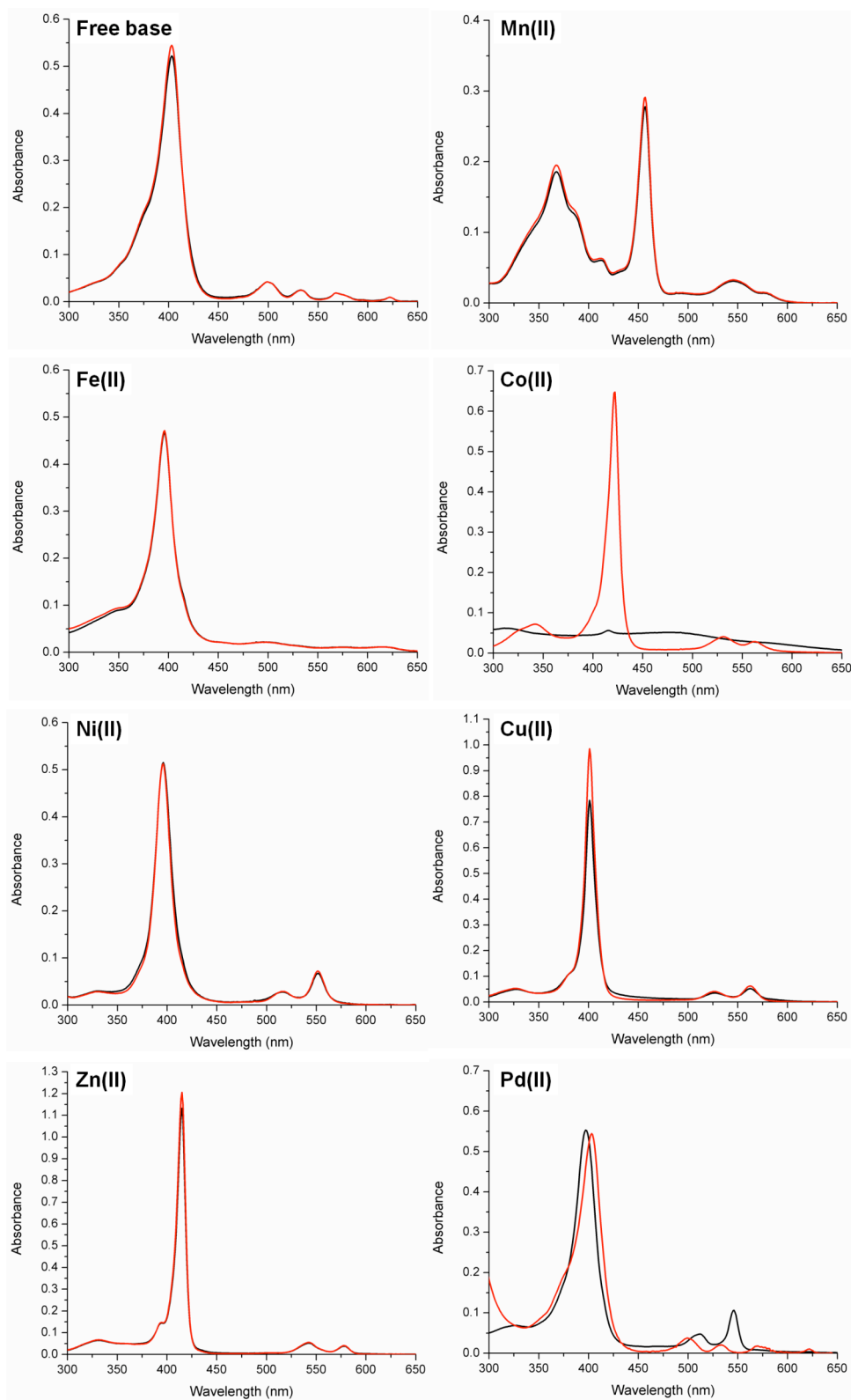


Figure S7. Absorption spectra (in DMSO) for metalation of uroporphyrin in aqueous solution under the reaction conditions listed in Table 2. Reactions in the absence (black line) or the presence of imidazole (red line).

V. Multicomponent analysis (MCA)

Competition between metals for metalation of uroporphyrin was monitored by absorption spectroscopy using the multicomponent analysis (MCA) module. This software requires the measurement of a spectrum for each pure component (standard) that is present in the sample. Samples of each were obtained employing reaction conditions listed in Table 2. The absorption measurements were carried out in DMSO with a diode-array spectrophotometer. To quantitatively determine the concentration of each porphyrin in a mixture of porphyrins with overlapping regions in the spectra, the first derivative of the spectra was used to emphasize the spectral differences. The maximum likelihood method and a wavelength range from 300–700 nm were set up for calculation. The processed standards and the corresponding residuals are shown in Figure S8.

Control experiments were carried to evaluate the ability of the software to predict the concentration of the eight different uroporphyrins in a mixture. The uroporphyrin standards were measured as samples to verify the accuracy of the results (Table S2). Here, each porphyrin was used alone, and the MCA method was used to assess the concentration using the eight spectra in the database. In each case, the porphyrin was identified correctly and only trace quantities of each other porphyrin were assigned in the fitting procedure. The concentration calculated for the porphyrin employed in each case is displayed in bold **red** font in the table. For example, when the Zn(II)uroporphyrin was employed, the concentration was calculated to be 2.41×10^{-6} M (entry 7), and each other species was at most 5.63×10^{-9} M, which is at the 0.2% level.

Samples containing mixtures of known amounts of each uroporphyrin were also analyzed by MCA (Table S3). Three types of experiments were carried out.

(i) Approximately equimolar amounts of each of eight uroporphyrins. Here, the concentration employed is shown in parentheses, and the calculated amount is shown alongside without parentheses. Use of a mixture of ~ 1 μM of each of the 8 uroporphyrins resulted in deconvolution of the composite spectrum into the component parts, with $<20\%$ error for six uroporphyrins but 24% error for the Cu(II)uroporphyrin and 31% for the Co(III)uroporphyrin (entry 1). The absence of free base uroporphyrin gave $<7\%$ error for seven uroporphyrins (entry 2). At ~ 0.25 μM of each of 8 uroporphyrins, there was $<10\%$ error for six uroporphyrins, 15% error for the Ni(II)uroporphyrin, and 21% error for the Fe(III)uroporphyrin (entry 3). At ~ 0.9 μM of each of the 8 uroporphyrins resulted in $<5\%$ error for all uroporphyrins (entry 4).

In the next two types of experiments, the concentration of the uroporphyrin that was varied is indicated in the table in bold **blue** font in parentheses, with the calculated amount shown in the table in bold **red** font.

(ii) 2–4-fold increase in concentration of 1–4 uroporphyrins in a mixture containing eight uroporphyrins (in otherwise approximately equimolar quantities), as shown in entries 4–8. In this experiment, the initial concentration of each of the 8 uroporphyrins was ~ 0.9 μM ($<5\%$ error for all uroporphyrins; entry 4). The concentration was then increased 2-fold for the Zn(II)uroporphyrin, 3-fold for the Ni(II)uroporphyrin, 4-fold for the Mn(III)uroporphyrin, and 2-fold for the Fe(III)uroporphyrin. Deconvolution of the composite spectra into the component parts gave $<14\%$ error for the 8 uroporphyrins.

(iii) $1/10^{\text{th}}$ the amount of one uroporphyrin in the presence of seven other uroporphyrins (in approximately equimolar quantities), as shown in entries 9–16. In general, the concentration of the uroporphyrin present in trace quantities was calculated with considerable error. The error was $<16\%$ for each of the seven uroporphyrins. In the case of the uroporphyrin with 10-fold lower concentration (0.1 or 0.05 μM) than the other seven uroporphyrins, the error was $<24\%$ for

the free base, Zn(II), Cu(II), Co(III), or Mn(III)uroporphyrin; 51% for the Ni(II)uroporphyrin; 40% error for the Pd(II)uroporphyrin; and 72% for the Fe(III)uroporphyrin. Note that the total amount of the uroporphyrin at $1/10^{\text{th}}$ that of all the rest is present at the 1.4% level.

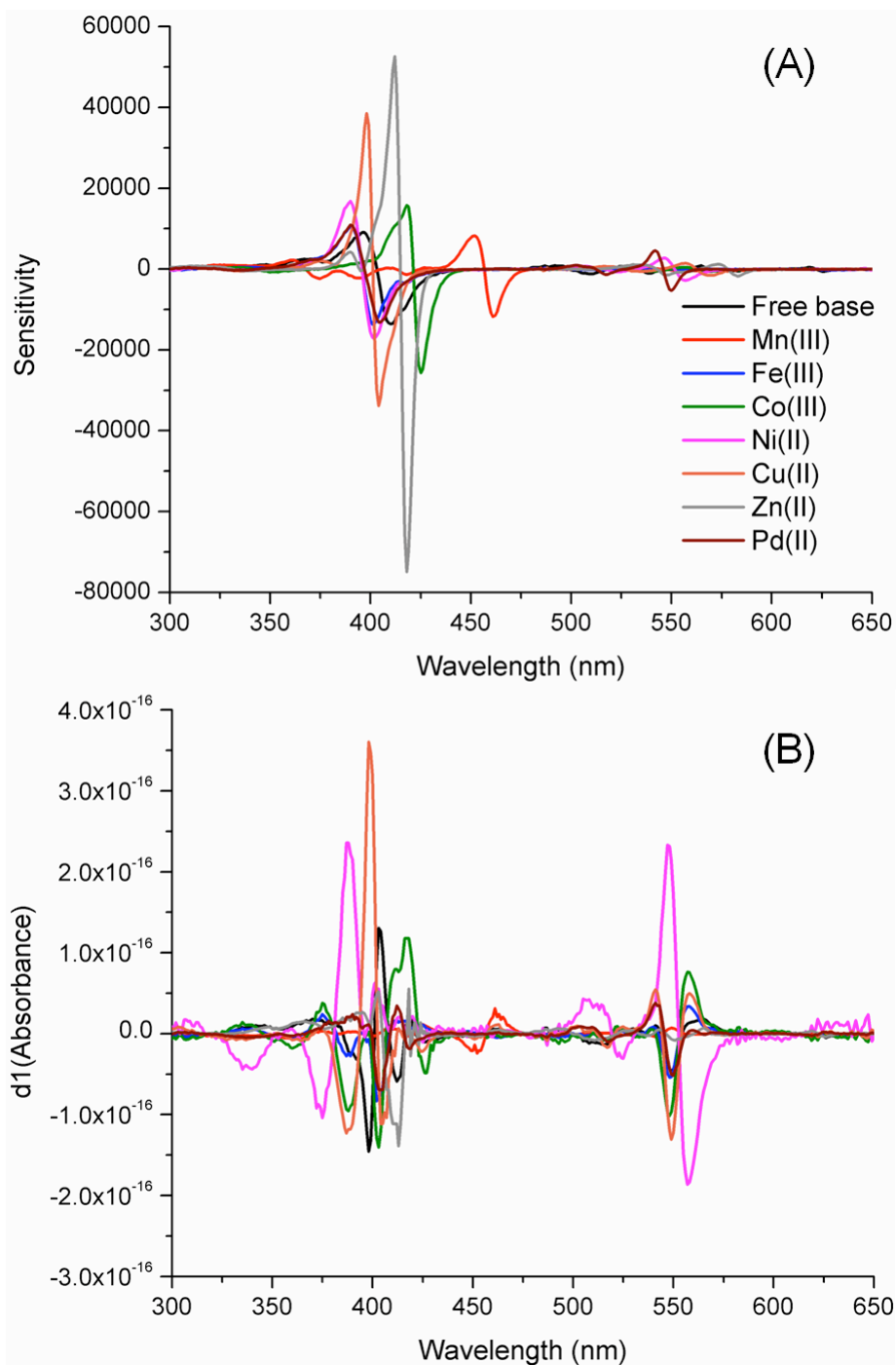


Figure S8. Spectra of the processed standards (A) and the corresponding residuals of processed standards (B). The labels in (A) denote the metalation state of the metallouroporphyrin employed.

Table S2. MCA validation, experimental set 1.

Entry	M-Uropor ^a	Concentration (M) of uroporphyrin of given metalation state ^b								
		Free base	Mn(III)	Fe(III)	Co(III)	Ni(II)	Cu(II)	Zn(II)	Pd(II)	Max. ^c
1	free base	2.48E-6	-1.32E-9	-1.65E-8	-1.58E-8	8.87E-9	6.82E-9	-8.91E-9	4.94E-9	2.32E-6
2	Mn(II)	3.37E-9	2.44E-6	7.22E-9	6.43E-10	-2.23E-9	-6.66E-10	-2.11E-11	-3.53E-9	2.45E-6
3	Fe(II)	-2.8E-9	8.87E-10	2.39E-6	1.83E-10	7.27E-9	4.67E-10	9.40E-10	1.86E-9	2.40E-6
4	Co(II)	-2.32E-9	9.38E-10	6.34E-11	2.43E-6	-4.33E-10	5.9E-10	4.32E-11	-9.47E-11	2.43E-6
5	Ni(II)	3.53E-9	-1.01E-9	1.64E-8	7.63E-11	2.45E-6	-6.99E-10	-3.78E-10	-5.3E-9	2.46E-6
6	Cu(II)	-4.5E-9	1.11E-9	5.34E-9	-7.96E-10	-4.61E-9	2.45E-6	-8.1E-12	-4.42E-10	2.44E-6
7	Zn(II)	3.45E-9	-1.91E-9	-5.63E-9	2.54E-9	5.63E-9	-1.99E-9	2.41E-6	-7.31E-10	2.43E-6
8	Pd(II)	-1.76E-8	1.76E-9	3.27E-8	-7.67E-10	-3.37E-8	4.46E-9	5.32E-10	2.47E-6	2.44E-6

^aMetal for metallouroporphyrin examined.

^bConcentration of each (metallo)uroporphyrin calculated by absorption spectroscopy using the MCA module. See text for color scheme.

^cMaximum concentration of each uroporphyrin in the sample.

Table S3. MCA validation, experimental set 2.

Entry	Concentration (x 10 ⁻⁷ M) of uroporphyrin of given metalation state ^a							
	Free base	Mn(III)	Fe(III)	Co(III)	Ni(II)	Cu(II)	Zn(II)	Pd(II)
1	11.06 (9.51)	12.10 (10.00)	9.39 (9.84)	14.56 (9.96)	11.82 (10.10)	13.26 (10.00)	10.17 (9.96)	9.78 (10.00)
2	-0.14 (0)	9.80 (10.00)	10.21 (9.84)	10.25 (9.96)	9.92 (10.10)	10.80 (10.00)	9.97 (9.96)	9.71 (10.00)
3	2.37 (2.50)	2.59 (2.59)	3.05 (2.40)	2.64 (2.59)	2.08 (2.45)	2.57 (2.45)	2.26 (2.50)	2.39 (2.50)
4	8.90 (9.26)	9.05 (9.17)	9.70 (9.27)	9.06 (9.26)	9.04 (9.25)	9.60 (9.25)	8.80 (9.25)	9.00 (9.25)
5	8.04 (9.18)	9.12 (9.09)	9.93 (9.18)	8.95 (9.18)	8.86 (9.16)	9.81 (9.16)	17.36 (18.33)	8.98 (9.17)
6	8.47 (8.92)	34.38 (35.34)	9.50 (8.93)	8.68 (8.92)	8.77 (8.90)	9.49 (8.90)	16.54 (17.82)	8.57 (8.91)
7	8.89 (8.76)	33.66 (34.71)	9.64 (8.77)	8.37 (8.76)	25.47 (26.23)	9.07 (8.75)	16.15 (17.50)	8.23 (8.75)
8	8.52 (8.68)	33.35 (34.40)	19.35 (19.10)	8.35 (8.68)	25.18 (26.01)	9.24 (8.67)	15.96 (17.35)	8.25 (8.67)
9	0.76 (1.00)	9.94 (9.92)	11.01 (10.02)	10.00 (10.01)	9.49 (10.00)	10.4 (10.00)	9.52 (10.00)	9.69 (10.00)
10	4.49 (4.83)	4.72 (4.81)	5.37 (4.86)	4.83 (4.85)	4.45 (4.82)	5.17 (4.82)	0.42 (0.48)	4.66 (4.83)
11	4.75 (5.01)	5.02 (4.98)	5.56 (5.04)	4.97 (5.03)	4.58 (5.00)	0.51 (0.49)	4.65 (5.00)	4.75 (5.00)
12	4.76 (5.01)	5.10 (4.98)	5.66 (5.04)	5.11 (5.03)	0.24 (0.49)	5.32 (5.00)	4.69 (5.00)	4.88 (5.00)
13	4.68 (4.83)	4.82 (4.81)	5.77 (4.87)	0.56 (0.50)	4.31 (4.83)	5.02 (4.83)	4.44 (4.83)	4.53 (4.83)
14	4.60 (5.01)	0.58 (0.52)	5.44 (5.04)	5.01 (5.03)	4.69 (5.00)	5.24 (5.00)	4.50 (5.00)	4.69 (5.00)
15	4.68 (5.01)	4.91 (4.98)	5.56 (5.04)	5.06 (5.03)	4.64 (5.00)	5.21 (5.00)	4.48 (5.00)	0.32 (0.50)
16	4.71 (5.01)	4.90 (4.98)	1.69 (0.48)	5.02 (5.03)	4.44 (5.00)	5.12 (5.00)	4.54 (5.00)	4.64 (5.00)

^aThe concentration of each (metallo)porphyrin was calculated by absorption spectroscopy using the MCA module. The amount of each uroporphyrin added to the sample is given in parenthesis. See text for color scheme.

VI. Dione–aminoketone reaction in the presence of each metal individually

The reaction of **1-AcOH** and **ALA** (120 mM of each reactant) was carried out in neutral aqueous solution (0.5 M MOPS buffer) at 60 °C for 24 h in the presence of 7.2 mM of each metal individually [M = Mg(II), Mn(II), Fe(II), Co(II), Ni(II), Cu(II), Zn(II) and Pd(II)], followed by illumination in the presence of 1,2-naphthoquinone-4-sulfonate (**NQS**).

A flowchart for reaction analysis is provided in Figure S9.

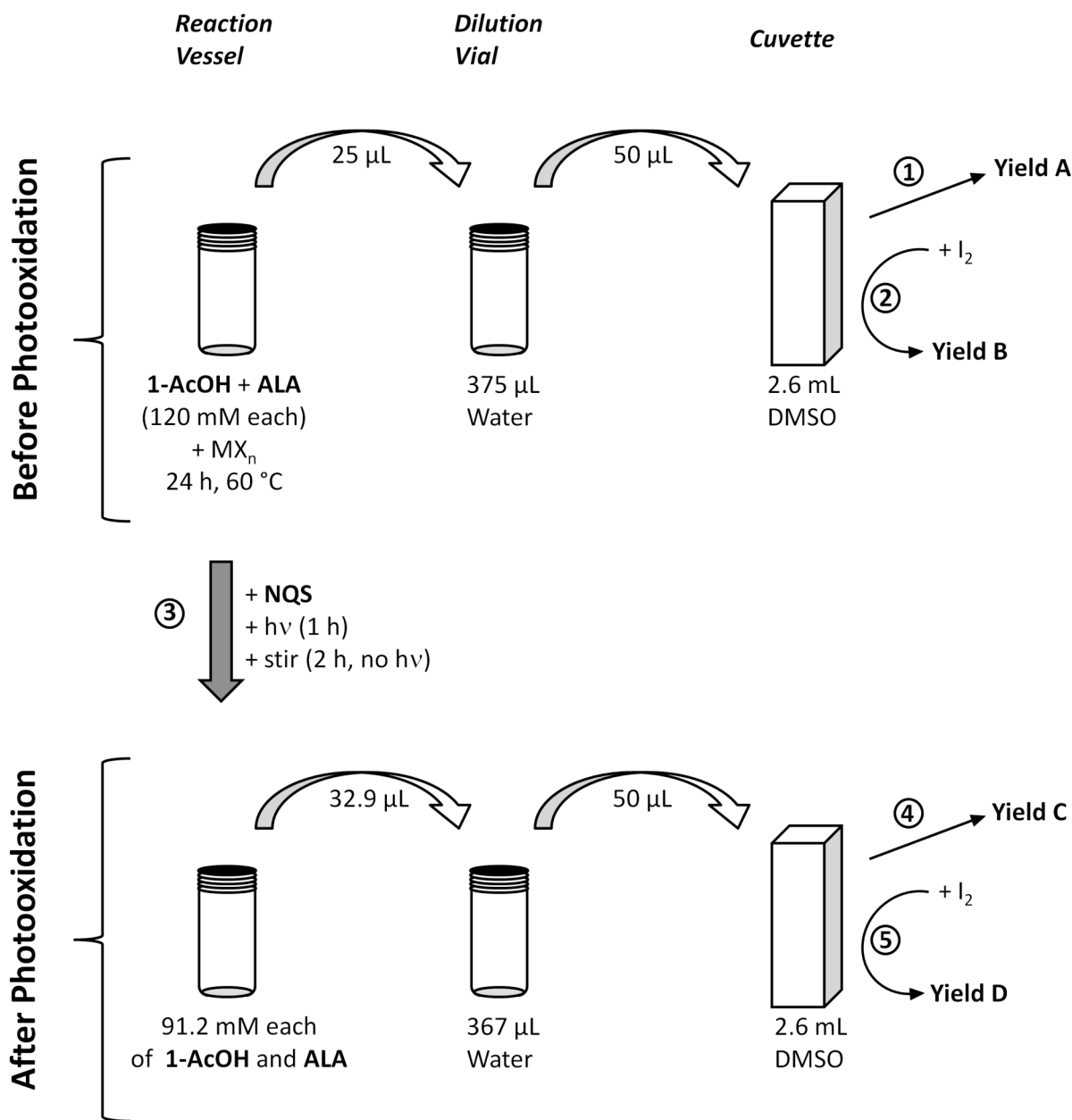


Figure S9. Experimental flowchart for the yield determinations in the reaction of **1-AcOH** and **ALA** in the presence of metals.

Before photooxidation: the reaction of **1-AcOH** and **ALA** was carried out in the presence of metals under anaerobic conditions for 24 h at 60 °C. To investigate the influence of metals in the formation of the macrocycle, an aliquot of the crude reaction mixture (prior to any deliberate

oxidation) was analyzed by absorption spectroscopy (step 1, **Yield A**). Subsequent treatment of the sample in the cuvette with I₂ was performed to achieve complete oxidation, thereby determine the overall porphyrin yield (step 2, **Yield B**) and verify the influence of metals in the overall process. The spectra are displayed in Figure S10.

After photooxidation: the crude reaction mixture was treated with 15 mM of **NQS** and illuminated for 1 h at room temperature under anaerobic conditions (step 3). The reactions were then stirred for 2 h without illumination and analyzed by absorption spectroscopy (step 4, **Yield C**). Chemical oxidation with I₂ of the sample in the cuvette was then performed to oxidize any remaining hydrophyrin species (step 5, **Yield D**). The spectra are displayed in Figure S11. Photographs of the samples in the dilution vials before and after photooxidation are provided in Figure S12.

One noteworthy point is that upon chemical oxidation (I₂) in the cuvette, any new porphyrin formed was necessarily a free base porphyrin given the dilute solution.

Examination of the quantity of NQS. The concentration of **NQS** was examined to identify suitable conditions for the oxidation of the uroporphyrinogens to give uroporphyrins. Similar results were obtained for the range of concentration analyzed (Table S4).

Table S4. Data for the photooxidation of uroporphyrinogens (from the reaction of **1-AcOH** + **ALA**) in the presence of **NQS**

NQS (mM)	Yield (%)			Percentage of oxidation (%) ^c
	Before photooxidation ^a	After photooxidation ^b		
	Crude rxn (Yield A)	Crude rxn (Yield C)	After I ₂ (Yield D)	
0	0	0.5	10.6	4.7
15	0	12.5	12.8	98
30	0	12.9	12.9	100
45	0	12.6	13.0	97

^aEach reaction contains 120 mM of each reactant and was carried out for 24 h at 60 °C.

^bThe reactions were treated with 0, 15, 30 or 45 mM of **NQS** and illuminated with the solar simulator using an AM0 D filter for 1 h.

^cPercentage of oxidation in the crude reaction following photooxidation versus that upon subsequent chemical oxidation (with I₂).

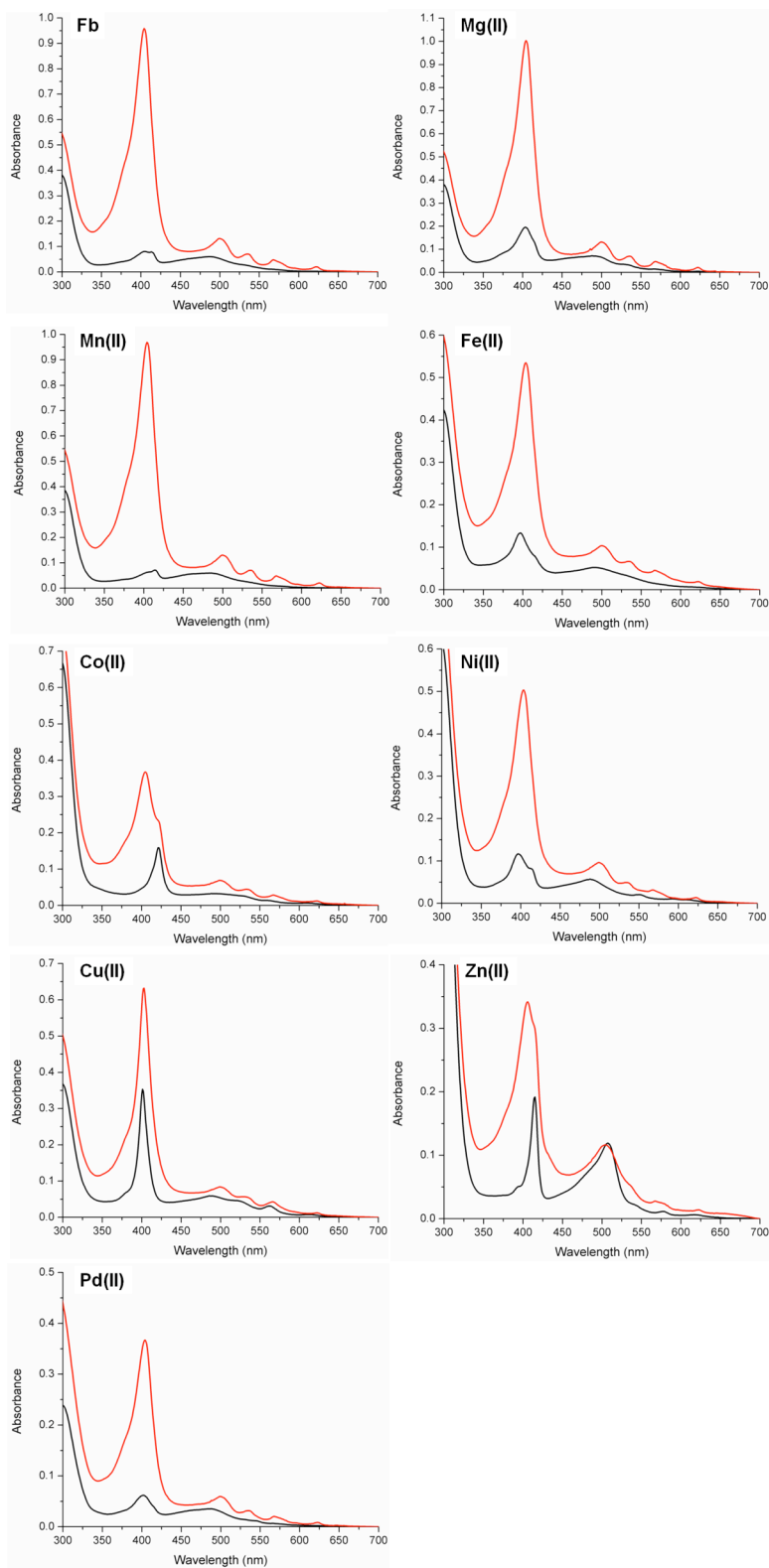


Figure S10. Absorption spectra (in DMSO) for the aqueous reaction of **1-AcOH** and **ALA** in the presence of each metal individually. Reaction before photooxidation (Yield A, black line) followed by I₂ oxidation (Yield B, red line).

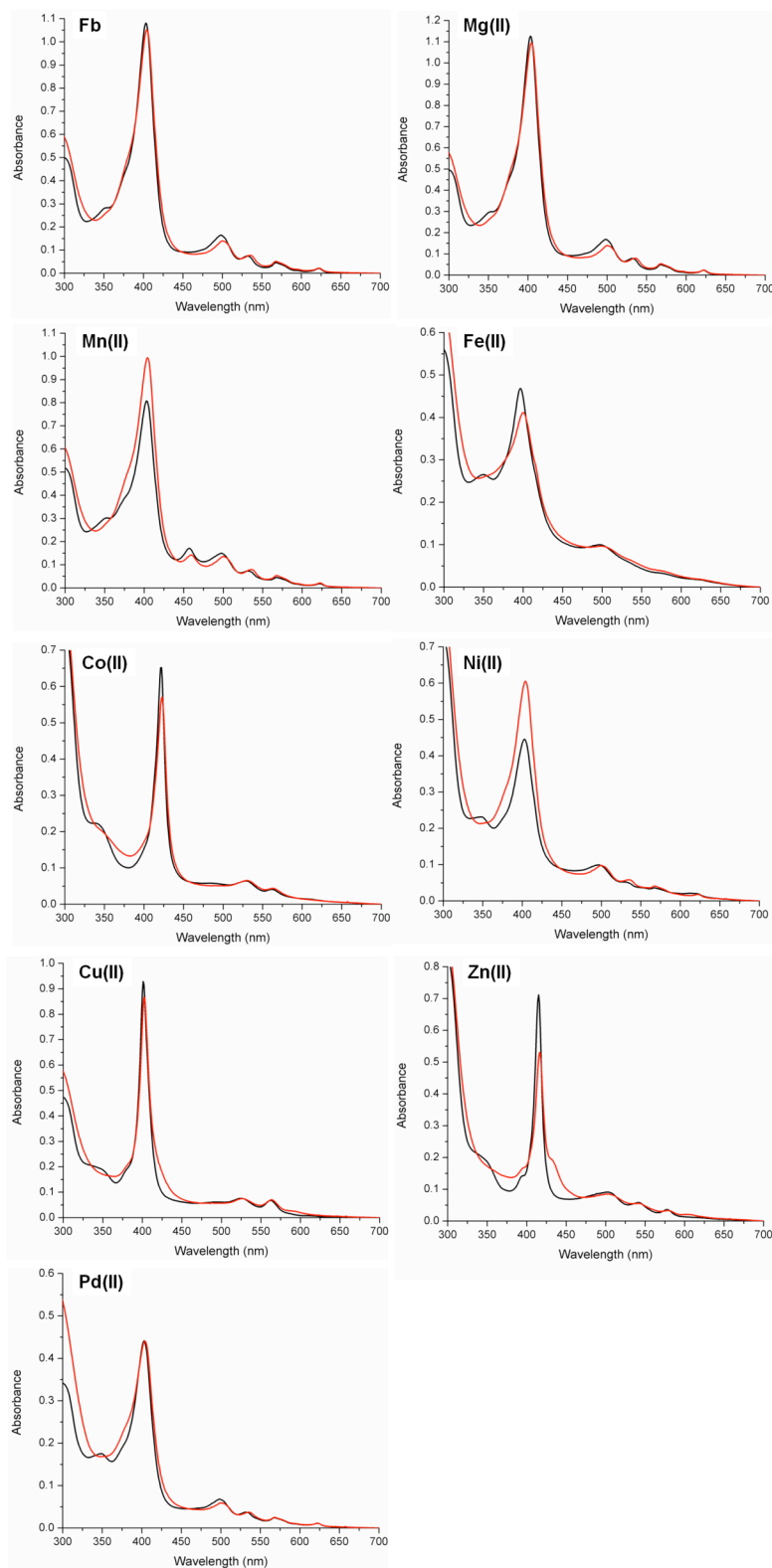


Figure S11. Absorption spectra (in DMSO) for the aqueous reaction of **1-AcOH** and **ALA** in the presence of each metal individually. Reaction after photooxidation (Yield C, black line) followed by I₂ oxidation (Yield D, red line).

Table S5. Spectral properties (Soret band only) and estimated yields for the reaction of **1-AcOH** and **ALA** in the presence of each metal individually.^a This is a full version of Table 4 (columns Yield A and Yield C are shown in the main text).

Metal	Before photooxidation ^b		After photooxidation ^c	
	Yield A (%) Crude (λ_{Soret} , M/Fb) ^d	Yield B (%) I ₂ oxidation (λ_{Soret} , M/Fb)	Yield C (%) Crude (λ_{Soret} , M/Fb)	Yield D (%) I ₂ oxidation (λ_{Soret} , M/Fb)
None	0.8 (405, Fb)	11.5 (404, Fb)	12.3 (403, Fb)	12.4 (404, Fb)
Mg(II)	2.0 (403, Fb)	12.1 (404, Fb)	12.9 (403, Fb)	13.1 (403, Fb)
Mn(II)	0.6 (405, Fb)	11.7 (404, Fb)	8.4 (403, Fb) 2.1 (457, M)	11.3 (404, Fb) 1.4 (459, M)
Fe(II)	1.3 (397, M)	5.8 (404, Fb)	4.4 (397, M)	3.7 (400, M)
Co(II) ^e	1.6 (421, M)	3.9 (405, Fb) 1.9 (422, M)	6.6 (422, M)	5.9 (423, M)
Ni(II)	1.0 (397, M)	5.6 (404, Fb)	4.1 (403, Fb)	6.4 (404, Fb)
Cu(II)	2.9 (401, M)	7.4 (403, Fb)	7.4 (401, M)	7.1 (402, M)
Zn(II)	1.0 (415, M)	3.5 (406, Fb)	4.0 (415, M)	3.0 (416, M)
Pd(II)	0.6 (402, Fb)	4.1 (404, Fb)	4.6 (403, Fb)	4.8 (404, Fb)

^aEstimated yields are based on the absorption at the Soret band maximum (collected in DMSO).

^bEach reaction (120 mM of each reactant) was carried out for 24 h at 60 °C in neutral aqueous solution in the presence of 7.2 mM of a metal salt. ^cThe reactions were treated with 15 mM of NQS and illuminated with the solar simulator using an AM0 D filter for 1 h, and then stirred for 2 h without illumination. ^dThe λ_{Soret} is given in nm; the “M/Fb” refers to the assignment of the spectrum to the metal chelate (M) or free base (Fb) species. ^eReaction carried out in the presence of imidazole (0.2 M).

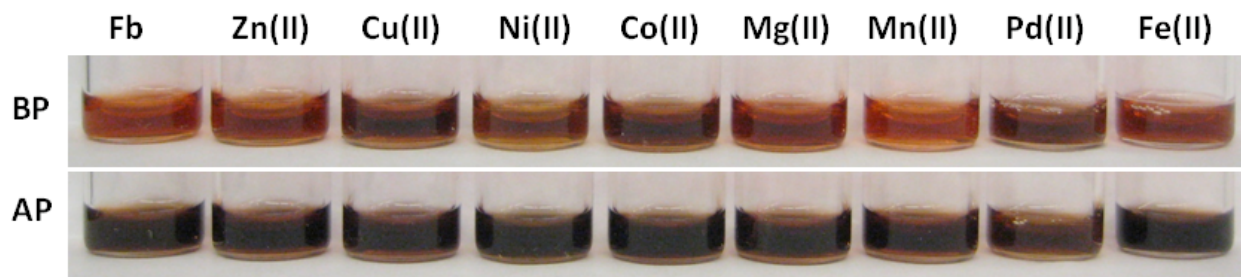


Figure S12. Photographs of dione–aminoketone reactions in the dilution vials. Legend: BP denotes before photooxidation (i.e., the samples used to generate yield A); AP denotes after photooxidation (i.e., the samples used to generate yield C).

VII. Examination of increased Mn(II)

Reactions of **1-AcOH** and **ALA** were carried out in the presence of increasing amounts of Mn(II). The concentration of Mn(II) ranged from 7.2 mM (2 equiv) to 28.8 mM (8 equiv). The yields of uroporphyrins are listed in Table S6 and the corresponding absorption spectra are shown in Figures S13-S14. We observed that the extent of metalation increased as the concentration of metal increased, yet the overall yield decreased. Also, the yield of free base uroporphyrins following photooxidation was lower than that upon chemical oxidation (I₂) for reactions with 4 and 8 equivalents of Mn(II).

Table S6. Spectral properties (Soret band only) and estimated yields for the reaction of **1-AcOH** and **ALA** in the presence of Mn(II)^a

[MX _n], mM	Before photooxidation ^b		After photooxidation ^c		% oxidation ^e
	Yield A (%) Crude (λ _{Soret} , M/Fb) ^d	Yield B (%) I ₂ oxidation (λ _{Soret} , M/Fb)	Yield C (%) Crude (λ _{Soret} , M/Fb)	Yield D (%) I ₂ oxidation (λ _{Soret} , M/Fb)	
0	1.4 (404, Fb)	8.6 (404, Fb)	9.9 (403, Fb)	10 (404, Fb)	99
7.2 (2 equiv)	1.0 (404, Fb) 1.2 (457, M)	6.3 (404, Fb)	6.4 (403, Fb) 1.4 (458, M)	6.8 (404, Fb) 1.2 (460, M)	94
14.4 (4 equiv)	1.0 (404, Fb) 1.8 (457, M)	6.4 (404, Fb)	4.0 (403, Fb) 2.8 (457, M)	6.6 (404, Fb) 2.3 (460, M)	61
28.8 (8 equiv)	0.6 (404, Fb) 1.5 (457, M)	5.9 (404, Fb)	2.1 (405, Fb) 3.2 (458, M)	5.1 (404, Fb) 2.6 (460, M)	41

^aEstimated yields are based on the absorption at the Soret band maximum (collected in DMSO).

^bEach reaction (120 mM of each reactant) was carried out for 24 h at 60 °C in neutral aqueous solution in the presence of 7.2, 14.4 or 28.8 mM of a metal salt.

^cThe reaction mixtures were treated with 15 mM of **NQS** and illuminated with the solar simulator using an AM0 D filter for 1 h, and then stirred for 2 h without illumination.

^dThe λ_{Soret} is given in nm; the “M/Fb” refers to the assignment of the spectrum to the metal chelate (M) or free base (Fb) species.

^ePercentage of formation of the free base uroporphyrins in the crude reaction mixture following photooxidation versus that upon subsequent chemical oxidation (with I₂), obtained by (Yield C)/(Yield D) x 100.

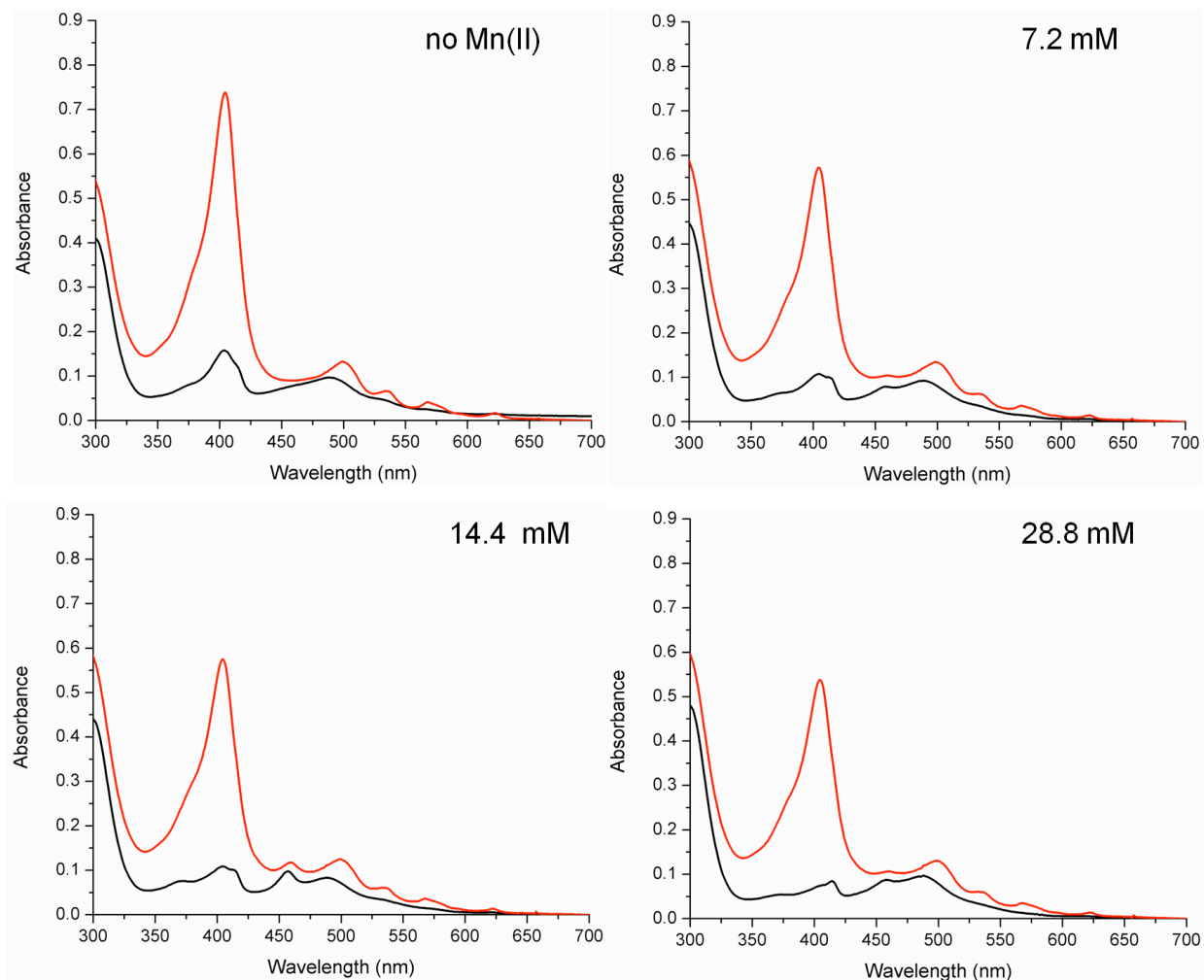


Figure S13. Absorption spectra (in DMSO) for the aqueous reaction of **1-AcOH** and **ALA** in the presence of Mn(II) in the amount indicated. Reaction before photooxidation (Yield A, black line) followed by I₂ oxidation (Yield B, red line).

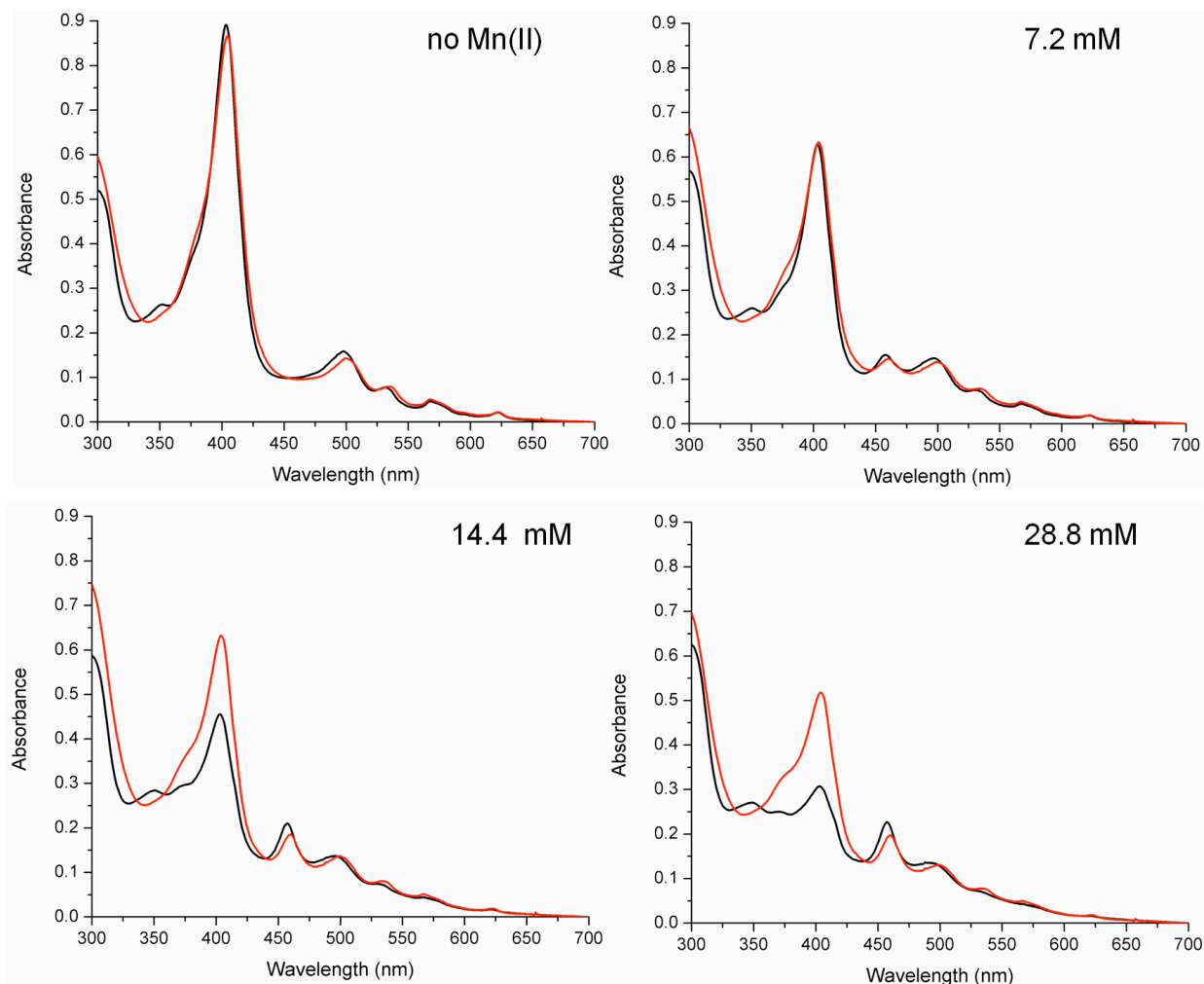


Figure S14. Absorption spectra (in DMSO) for the aqueous reaction of **1-AcOH** and **ALA** in the presence of **Mn(II)** in the amount indicated. Reaction after photooxidation (Yield C, black line) followed by I_2 oxidation (Yield D, red line).

VIII. Dione-aminoketone reaction in the presence of a mixture of metals

Reaction of **1-AcOH** and **ALA** was performed in the presence of 7.2 mM in total of a mixture of metals [i.e., **Mg(II)**, **Mn(II)**, **Fe(II)**, **Co(II)**, **Ni(II)**, **Cu(II)**, **Zn(II)** and **Pd(II)**]. The absorption spectra before and after photooxidation are shown in Figures S15. Due to the complex nature of the reaction mixture, the sample after photooxidation was analyzed by MALDI-MS (Figure S16, panel B) and compared to that from an equimolar mixture of free base uroporphyrin and metallouroporphyrins [$M = \text{Mn(II)}$, Fe(II) , Co(II) , Ni(II) , Cu(II) , Zn(II) and Pd(II)] (Figure S16, panel A).

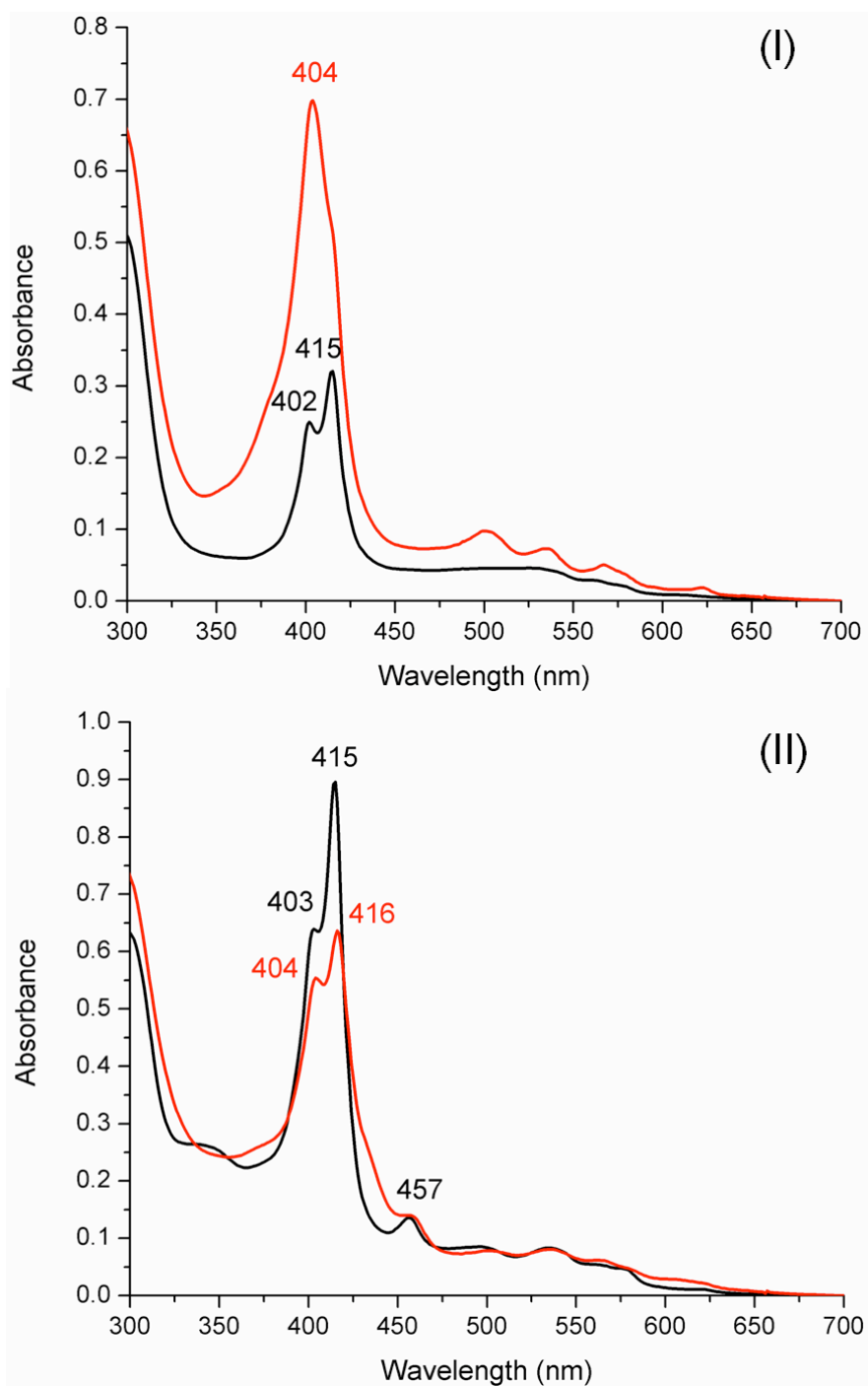


Figure S15. Absorption spectra (in DMSO) for the aqueous reaction of **1-AcOH** and **ALA** in the presence of a mixture of metals. (I) Reaction before photooxidation (Yield A, black line) followed by I_2 oxidation (Yield B, red line). (II) Reaction after photooxidation (Yield C, black line) followed by I_2 oxidation (Yield D, red line).

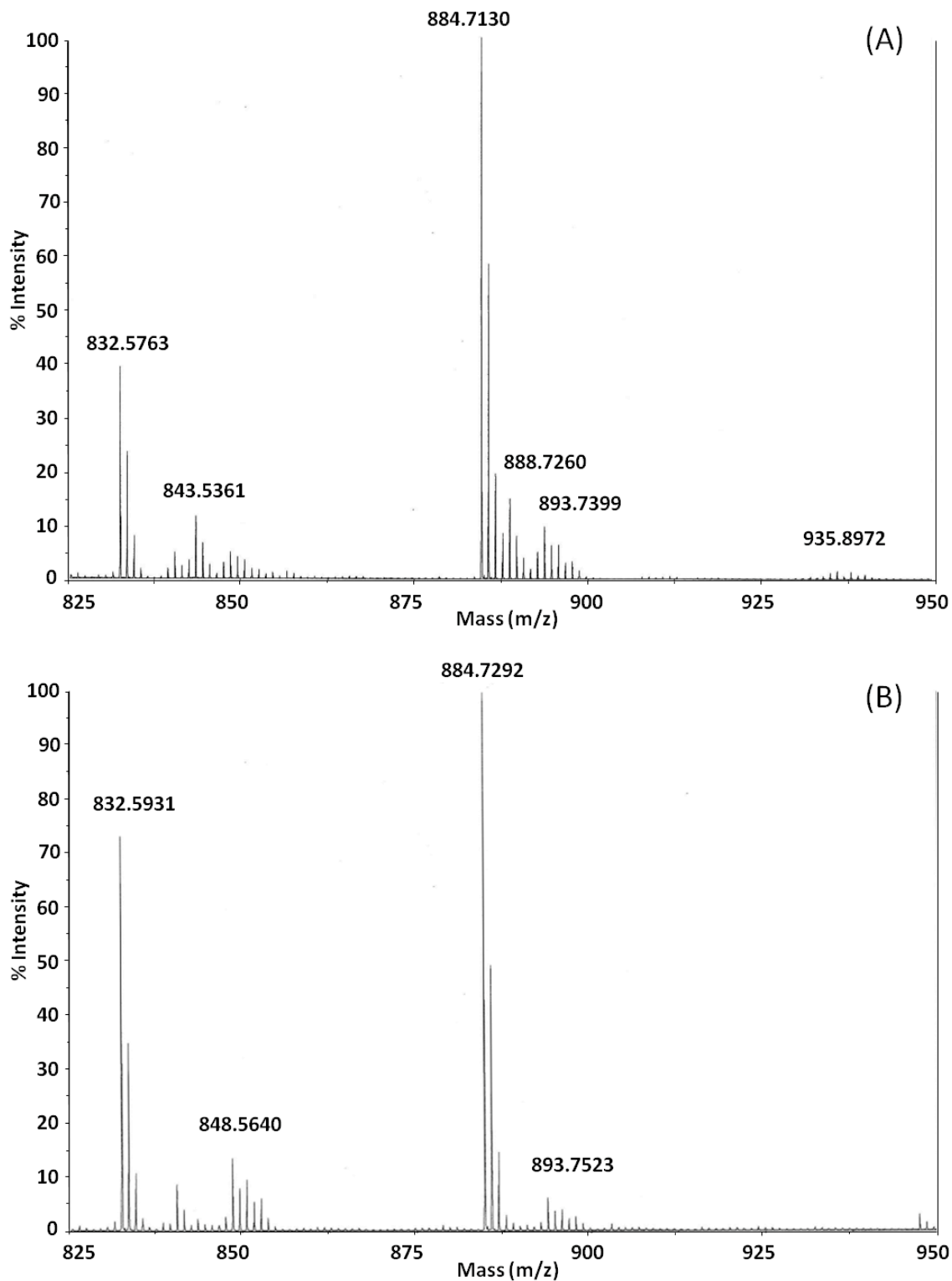


Figure S16. MALDI-MS data for a mixture of (metallo)uroporphyrins. (A) Spectrum of a mixture of (metallo)uroporphyrin standards. (B) Dione-aminoketone reaction in the presence of the mixture of metals.